Effect of Maleic Anhydride Grafting on Nanokaolinclay Reinforced Polystyrene/High Density Polyethylene Blends

Tresa Sunitha George,[1,2] Asha Krishnan,[1] Newly Joseph,[1] R. Anjana,[1,3] K.E. George[1]
[1]*Department of Polymer Science and Rubber Technology, Cochin University of Science and Technology, Cochin 682022, Kerala, India*

[2]*Department of Chemistry, St. Pauls College, Kalamassery, Kerala, India*

[3]*Department of Chemical Engineering, Government Engineering College, Thrissur, Kerala, India*

Nanofillers have revolutionized the field of polymer modification. Modification of polymer blends with nanofillers opens up a myriad of opportunities to develop materials of choice. Polystyrene (PS) and high density polyethylene (HDPE) are two widely used standard plastics. To generate high modulus and strength a PS rich blend of PS/HDPE (80/20) was selected and the blend was modified using low cost nanokaolin clay, a 1:1 alumina silicate. The effect of maleic anhydride grafted PS/PE as compatibilizer in this system was studied. The incorporation of the compatibilizer improves the mechanical properties. This can be correlated with better interfacial adhesion as evidenced by scanning electron microscopy. The optimum in these properties was obtained at a compatibilizer concentration of 10–15%. The composites were characterized by X-ray diffraction, differential scanning calorimetric, and dynamic mechanical analyzer techniques. This study shows that kaolin can be used as potential modifier of PS/HDPE blend. POLYM. COMPOS., 00:000–000, 2012. © 2012 Society of Plastics Engineers

INTRODUCTION

Polymer nanocomposites are a class of hybrid materials composed of an organic polymer matrix that is imbedded with inorganic particles, which have at least one-dimension in the range of 1 to 100 nm [1]. Polymer nanocomposites have attracted great interest, because they exhibit enhanced mechanical, thermal, and barrier properties [2]. Particular interests are nanocomposites consisting of organically modified layered silicates because they often exhibit remarkable properties when compared with those of virgin polymer [3].

Polystyrene (PS) and high density polyethylene (HDPE) are two of the most widely used standard plastics in the world. The modification of PS/HDPE blends with nanofillers may generate a variety of materials for commercial applications. Commercial success of an immiscible blend requires improvement of interfacial adhesion between the components of blends, necessary to achieve stability of morphology and improvement in mechanical properties. PS is incompatible with HDPE. Therefore, PS/HDPE blends exhibit weak interfacial adhesion and poor dispersion of the component, which results in heterogeneous morphology with macro phase separation and poor mechanical properties. PS and poly methyl methacrylate are two examples of high modulus materials that have limited impact resistance, whereas polyethylene and polypropylene are two tough materials that have poor stiffness. An increase in impact strength of PS can be achieved by adding HDPE, which is having high impact strength [4, 5]. For this reason PS/HDPE blends exhibit more balanced properties, which is advantageous for a number of applications, e.g., in packaging where different barrier properties of HDPE and PS can be beneficially combined. The PS/HDPE blends are very important for mixed plastic waste recycling [6]. The present trend in reducing the municipal solid waste is to recycle the polymer waste instead of incineration and land filling [7].

Blending of a second component has been suggested as a method to improve the dispersion of nanoclay in polymer melts [8]. The tendency of nanoclay to be localized at the interface of the multiphase system improves their homogenous dispersion. The surface energy at the interface between two phases improves clay dispersion

Correspondence to: Tresa Sunitha George or K.E. George; e-mail: sunithariju@gmail.com or kegeorge@cusat.ac.in
DOI 10.1002/pc.22276
Published online in Wiley Online Library (wileyonlinelibrary.com).
© 2012 Society of Plastics Engineers

[9]. This blending method has been suggested as a way to compatibilize immiscible polymer blends such as PP/PS, EVA/PP, and PE/PBT [10]. Organically modified nanoclays (organoclay) frequently exhibit a synergic effect on the blend morphology beyond the reinforcing effect in a blend. [8, 9, 11–14]. The size of the nanoclay particles, the modifications incorporated, and the amount nanofiller used play a major role in the development of properties of polymer blends [15]. The majority of these studies have employed layered, anionic phyllosilicates as the organic component owing to their high aspect ratio and ease of ionic modification. As the natural deposits of montmorillonite minerals are rather limited, and as the demand for bentonites is ever increasing, there has been considerable investigation for finding substitute products for this type of products [16]. In this context, only scanty data is available with the relatively less expensive and abundantly available mineral kaolin [17]. It was observed in a recent report that the clay–polymer nanocomposite prepared from china clay-based nanoclay gives better oxygen barrier and water transport property than that from montmorillonite-based nanoclay [18]. Kaolinite has the potential to be an ideal precursor for the preparation of new nanocomposite materials since it is cost effective when compared to montmorillonite clays. Kaolinite has a greater theoretical internal surface area per unit mass than do the smectites (1000 m^2/g vs. 700 m^2/g), and it exhibits a much greater crystallinity than do the smectites. While smectites are widely used for the preparation of polymer layered silicate nanocomposites, a few examples of kaolinite-polymer intercalated nanocomposites have been reported [19–24]. The exploitation of other preparation techniques is still limited in case of polymer-kaolinite nanocomposites, although it is well explored in case of smectite precursors. Also, the number of polymers involved in nanocomposite interactions with kaolinite is still limited and not covering a wide variety of polymers. Nowadays, the most successful commercial uses of polymer–clay nanocomposites are probably in the car industry (weight reduction) and in food packaging (gas barrier properties) [25]. It must be outlined that the processing of polymer–clay nanocomposite [26] needs low loadings [typically between 1% and 5% (w/w)] when compared to conventional fillers [20–40% (w/w)].

The physical mixture of polymer and silicate may not always form a nanocomposite. It may rather separate into discrete phases. To improve dispersibility of nanofillers in polymer matrices grafted polymers are used as compatibilizers. Maleic anhydride (MA) is suitable for grafting because MA has low reactivity towards itself and it grafts onto the polymer. The hydroxyl group of clay can react with MA groups to disperse the nanofillers well within matrix polymer through *in situ* compatibilization. Comparatively, the organotreated nanoparticles can disperse more effectively than the untreated ones. The objective of the study is to upgrade PS/HDPE blend by using nano-kaolin clay to make the blend suitable for more demanding applications.

EXPERIMENTAL

Materials

PS (General purpose polystyrene) supplied by Supreme Petro Chem, Mumbai, India; MFI-12 gm/10 min (200°C/5 kg). HDPE (HD50MA180), Reliance Polymers, Mumbai, MFI 20 gm/190°C/2.16 kg). Nano kaolin clay-Nano caliber 100*M*, which is a Mercaptosilane modified clay supplied by English India Clays, India. MA and dicumyl peroxide (DCP) were supplied by LOBA-chem, Mumbai.

Preparation of the Compatibilizer and Its Characterization

The compatibilizer was prepared by grafting reaction between MA and a PS/HDPE blend in the presence of a DCP initiator at 180°C for 8 min. The reaction was conducted by melt mixing in a Thermo Haake Polylab system equipped with roller rotors. PS and HDPE were allowed to melt for 2 min initially. Then varying quantities of MA (0, 1, 1.5, 2, 2.5 wt%) were added at constant concentration of DCP to find the optimum amount of MA. The grafting reaction was monitored using soxhlet extraction. Samples were compressed into thin films, cut into small pieces, and then put into contact with acetone using soxhlet apparatus for 16 h to remove the unreacted MA. It was finally dried in a vacuum oven at 70°C for 12 h. The product before and after soxhlet extraction was weighed and percentage of grafting was determined.

Fourier Transform Infrared Spectroscopy (FTIR)

The grafting of MA on the blend was confirmed by the FTIR spectra recorded on a Thermo Nicolet FTIR Spectrometer Model Avatar 370. Samples in the form of thin films, <1 mm thickness, were employed.

Preparation of the Composites

PS/HDPE (80/20) blends were mixed with modified kaolin clay and the compatibilizer using a Thermo HAAKE Polylab system equipped with roller rotor operating at 180°C and 50 rpm for 8 min. The resulting compounds were hot pressed into sheets and cut into pieces. The material was then injection molded at 190°C. The blends are designated as follows-PB means a blend of 80% of PS and 20% HDPE. The blends containing clay were designated as PBX, where *X* is 1, 2, 3 wt% of clay(e.g., PB1) and MA-grafted polymer compatibilized blends were designated as PBXC, where *C* represents the wt% of compatibilizer 5, 10, 15, 20, 25 etc. (e.g., PB215).

 DOI 10.1002/pc

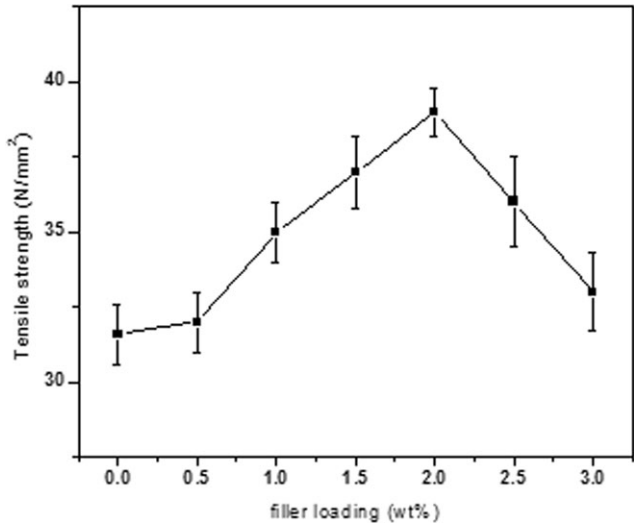

FIG. 1. Variation of tensile strength with filler loading.

Determination of Mechanical Properties

Tensile properties were evaluated using Shimadzu Autograph AG-1 series Universal testing machine with a load cell of 10 kN capacity according to IS0 527 on dumbbell shaped specimens.

X-Ray Diffraction (XRD)

Samples for X-ray diffractometer were analyzed in a Bruker AXS D8 Advance X-ray diffractometer.

Differential Scanning Calorimetric (DSC)

The samples were first heated under vacuum for 15 min at 85°C (elimination of water) before it was sealed in an aluminum pan with a perforated lid. The sample pan was placed in a DSC cell (Q-100, TA instruments calorimeter) under a dry nitrogen purge. The samples (5–10) mg were inserted into the apparatus and immediately heated from 50 to 250°C at a rate of 50°C/min and kept for 1 min at this temperature for erasing thermal history and then cooled to 50°C at a rate of 10°C/min kept isothermal for 1 min and then heated again to 250°C at a rate of 10°C/min.

Dynamic Mechanical Analyzer (DMA)

The storage modulus as a function of temperature was assessed by DMA using TA Q-800. Analyses were done using dual cantilever at 1 Hz frequency at a temperature range of 40–123°C at 3°C/min.

Scanning Electron Microscopy

SEM was used to investigate the morphology of the fractured surfaces. The fractured surface was sputter coated with gold and examined under SEM. SEM images were taken using a JOEL model JSM 6390LV.

RESULTS AND DISCUSSION

Mechanical Properties

Effect of Kaolin Clay. Figures 1 and 2 shows the variation of tensile strength and tensile modulus with kaolin clay at different loadings. The addition of fillers leads to a significant increase in mechanical properties. This is similar to the behavior reported earlier by Zhao et al. [27]. They observed the increase in tensile performance by the incorporation of nano TiO_2 in polypropylene. The improvement in mechanical properties continues up to a filler loading level of 2% and thereafter a slight decrease is observed. This may be due to good filler dispersion and effective interaction of nanoparticle at this composition. At higher particulate loading there is a tendency for nanoparticles to aggregate heavily. Svehlova et al. [28] has suggested that better filler dispersion leads to a higher modulus. Modulus is an indication of relative stiffness of composites. The modulus tends to increase with the volume fraction of fillers in every case, but in some systems there is a critical volume fraction at which aggregation occurs and the modulus goes down [29–31]. Hence, a higher mechanical performance of nanocomposite is an indication of better filler dispersion. The addition of kaolin clay seems to improve the stress transfer between both parts and results in improvement strength and modulus.

Figure 3 shows variation of elongation at break with clay loading. The change in strain to failure behavior of nanocomposite is different depending upon the system. In general addition of nanofillers to a moderately crystalline polymer regardless of filler matrix interaction reduces the maximum strain [32]. An opposite trend is found in amorphous polymers as in this case where PS composition is 80%. Elongation at break increases with increase in clay content up to 2% and decreases at higher concentrations, indicating that composites were becoming brittle on

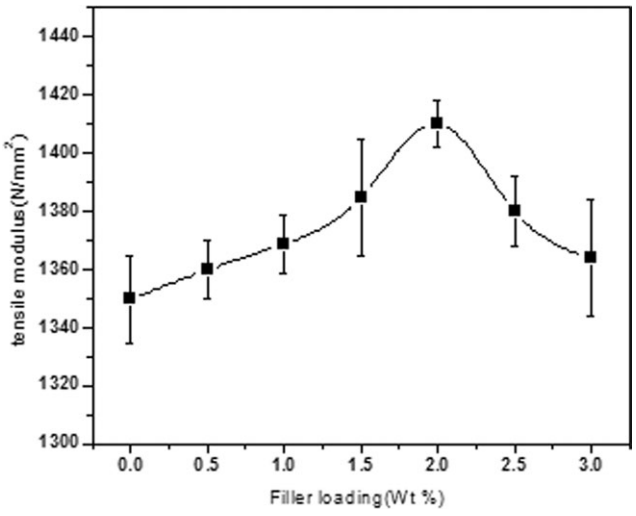

FIG. 2. Variation of tensile modulus with filler loading.

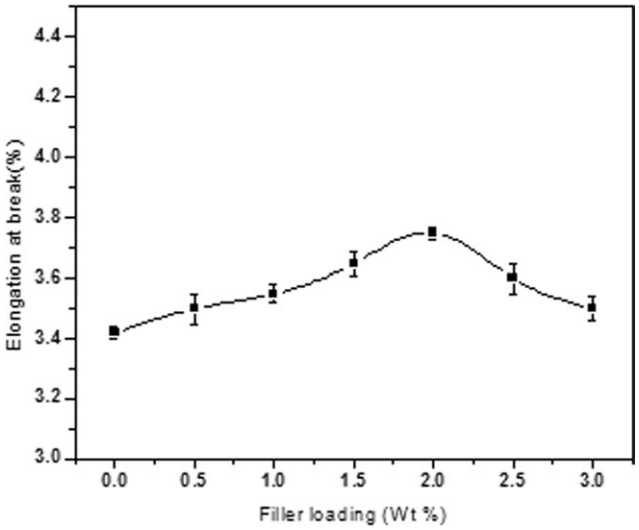

FIG. 3. Variation of elongation at break with filler loading.

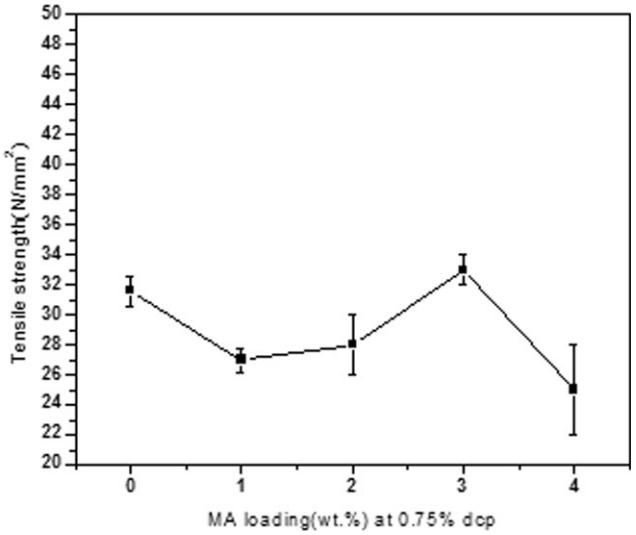

FIG. 4. Effect of ma content on tensile strength of PB.

higher loading. This suggests that adhesion of the filler particles on to the polymer matrix is strong and this induces a viscoelastic deformation and matrix yielding at 2%. With further increase of clay loading, the strain decreases because of the aggregation of kaolin [24]. The increase in elongation at break also shows that kaolin can also improve the impact toughness of the blend. This is consistent with the observations reported earlier [33].

Effect of MA Grafting. Figure 4 shows the effect of MA content on tensile strength in the presence of DCP. The variation in tensile strength is not substantial. The maximum tensile strength occurs at 3% MA loading and grafting yield is found to be 2.35%.

Effect of Compatibilizer Content. From the above data in Figs. 1 and 2, 2 wt% of kaolin clay is selected as optimum concentration for further studies. Figures 5–7 shows the effect of compatibilizer content on tensile strength, modulus, and elongation at break of PS/PE blends containing 2 wt% of kaolin clay. The tensile strength and tensile modulus increases with increasing percentage of compatibilizer up to 15% and then decreases. This may be because of the lower interfacial tension and enhanced interfacial adhesion of the compatibilized blends, making stress transfer more efficient between phases during fracture [34]. The improvement in tensile strength and tensile modulus is as much as 18% and 10% when compared with the pure blend (PB). The interfacial adhesion is increased by the presence of the compatibilizer and the high surface area of the filler gives rise to increased modulus and strength. Elongation at break also displays the same trend, which shows the ductile nature of composites on adding compatibilizer. When the composites are under exterior stress, the filler helps to distribute the stress evenly, and delays the rupture of the material [35]. Rong et al. observed a similar trend on comparing break strain of composites with SiO_2 nanoparticles in a polypropylene matrix with and without the addition of graft polymers [36].

FTIR

Figure 8 shows the FTIR spectra of the (a) PB and the (b) MA grafted composite. The peaks at 2912 and 2847 cm^{-1} represent the CH stretching modes in CH_3, CH_2 etc. The peaks at 1463 cm^{-1} (double bond region) and below 1000 cm^{-1} indicate the CH deformation of the substituted benzene ring of PS. The peak at 690 cm^{-1} represents the mono substituted benzene ring of PS. The peaks that appear in the range of 3500 and 3200 cm^{-1} may be due to the OH stretching in clay. The peak at 1729 cm^{-1}, which is assignable to symmetric stretching of C=O groups present in MAs. As per the "Rule of Three" peaks in the range of 1200 cm^{-1} (C—C—O),

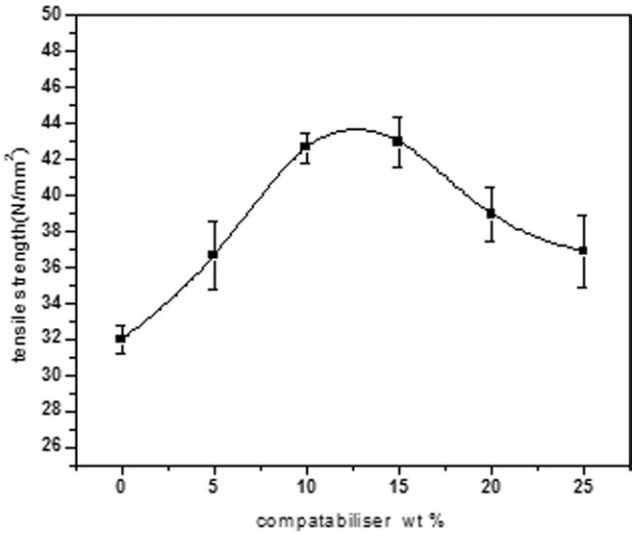

FIG. 5. Variation of tensile strength with compatibilizer loading.

DOI 10.1002/pc

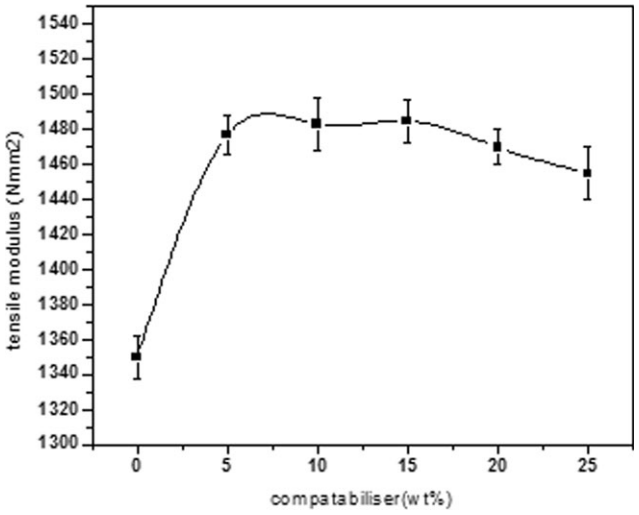

FIG. 6. Variation of tensile modulus with compatibilizer loading.

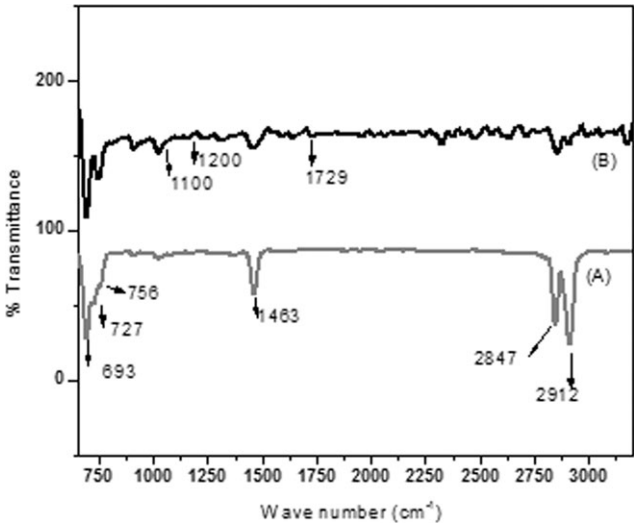

FIG. 8. FTIR of (a) PB and (b) grafted composite.

1100 cm^{-1} (O—C—C), together with a peak at 1729 cm^{-1} suggests the presence of ester groups in the grafted sample. The intensities of peaks at 2912, 2847, and 1463 cm^{-1} are reduced on addition of MA [37].

XRD

Figure 9 shows the XRD patterns in the range of $2\theta = 10°–50°$ for kaolin clay, the blend containing 2% kaolin clay PB2 and the compatibilized nanocomposite-PB215. The XRD pattern of kaolin clay shows characteristic reflection peaks at 2θ values of 12.243°, 19.9°, 21.2°, 24.8°, 34.9°, 35.8°, 38.3°, 45.4°, 55.1°, and 62.20° with respective d spacing (in nm) at 7.16, 4.45, 4.18, 3.58, 2.56, 2.50, 2.4, 1.99, 1.66, and 1.49. The peak at 12.243° indicates the d_{001} plane of the kaolin clay. On the other hand the diffractogram of the PB is also seen to show peaks at 21.208°, 23.58° with respective d spacing at 4.18 and 3.76, peaks almost similar to kaolin clay. Hence, nanocomposite prepared can be evaluated nicely by observing the peak at 2θ 12.2°, 35°, 38° etc. In PB2 a relatively small and inconspicuous peak is seen at 12.2° while all other peaks are absent. The nonappearance of Braggs scattering at 12.2° for PB215 reveals an expansion

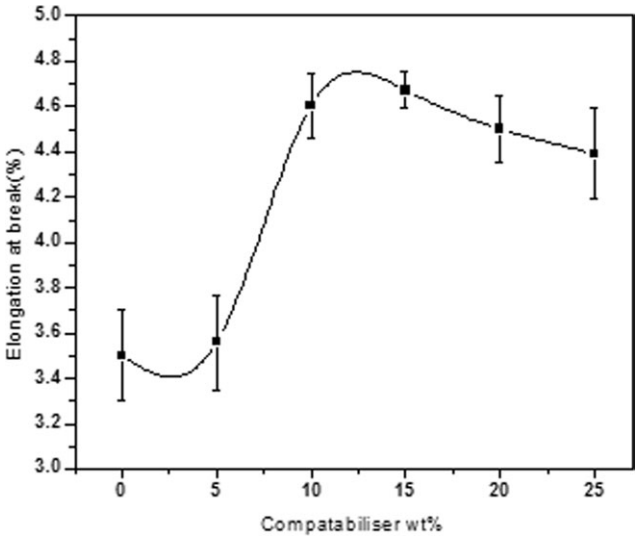

FIG. 7. Variation of elongation at break with compatibilizer loading.

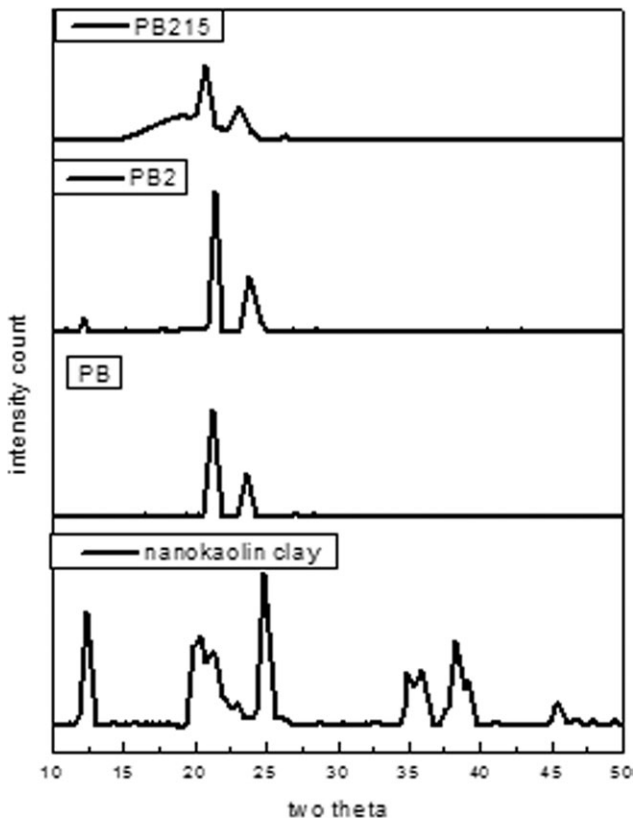

FIG. 9. XRD of clay and composites.

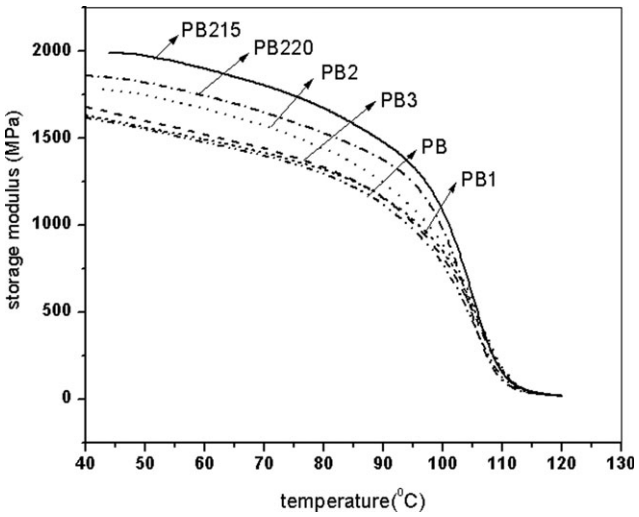

FIG. 10. DMA of composites.

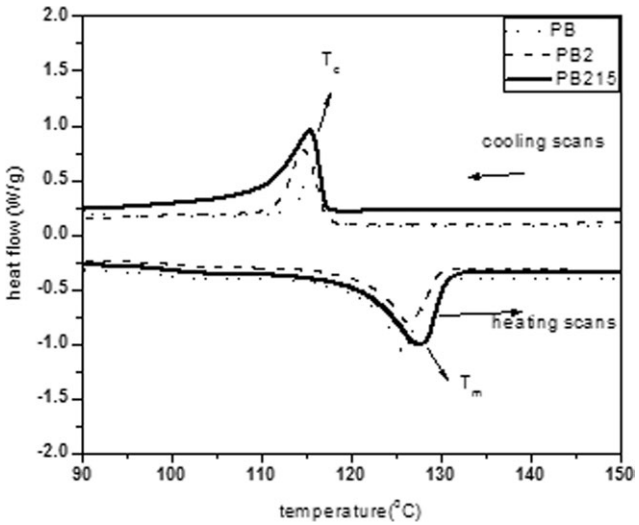

FIG. 11. DSC cooling and heating curves of composites.

of clay layers into the matrix. The XRD pattern of PB215 showed that on addition of the compatibilizer, clay is found to affect the crystallographic nature of the polymer matrix. This indicates that the polymer is able to intercalate into organoclay and increase the *d* spacing of clay galleries. Tang and Hu [38] attributed the absence of diffraction peaks to the delaminating of the clay. It has also been reported elsewhere that the disappearance or decrease of intensity of diffraction peaks could be attributed to the fact that the silicates are partially or completely exfoliated [39].

DMA

The dynamic storage modulus of the nanocomposite as a function of temperature at 1 Hz is shown in the Fig. 10. It shows steady decrease of modulus with increase in temperature. The storage modulus of the nanocomposite shows an increase at 2 wt% of kaolin clay, which indicates efficient stress transfer between the matrix and the filler. Kaolin clay at 3% shows a decrease in storage modulus, which may be due to agglomeration of the nanofiller above this percentage. The compatibilized blends show a significant increase in storage modulus. This shows that the MA groups present in the polymer backbone increase the interaction between the filler and matrix, causing an efficient stress transfer between matrix and clay. These results are consistent with the tensile modulus data, which also represent the relative stiffness of the samples.

DSC

The DSC thermograms (enthalpy vs. temperature) of PB, PB2, and PB215 are shown in Fig. 11. The figure depicts the exotherm crystallization peak and the endotherm peak of PB, PB2, and PBC215. The crystallization data (percentage crystallinity X_c, peak melting temperature T_{mp}, onset of melting temperature T_{mo}, and peak onset of crystallization temperatures T_{cp}, T_{co}) obtained for PB, PB2, PB215 are presented in Table 1. The effect of the compatibilizer on the PS is not explored, only crystallization and melting temperature of HDPE is shown. Since, PS is amorphous it does not have a sharp melting point nor crystallization temperature.

Because of the nucleation effects, it is assumed that, crystallization temperature, T_c of the nanocomposites would be higher than their corresponding neat blends [40–43]. However, the T_c of nanocomposites does not vary much in this case. This is in agreement with other reports [44, 45]. In this study the crystallization temperature, both onset (T_{co}) and peak (T_{po}) temperature of composites remains almost same. Recently, Perrin-Sarazin et al. [46] reported a decrease of crystallization temperature in the case of PP/PP-*g*-MA/clay intercalated nanocomposites. They noted that specific interactions between the MA groups of the coupling agent and clay particles could reduce the mobility of crystallizable chain segments, thus limiting the nucleating effect of the clay. This could provide an explanation for the variation in the crystallization temperature observed in the case of PS/HDPE composites. A considerable increase in peak melting temperature is observed in the case of nanocomposites.

SEM Morphology

Since, the mechanical properties, of the blends are influenced by the blend morphology as well as interfacial interaction between phases, the consideration of morphologies will be very valuable. The change in mechanical

TABLE 1. DSC thermogram data.

Material	T_{mo} (°C)	T_{mp} (°C)	H_m (J/g)	X_c (%)	H_c (J/g)	T_{co} (°C)	T_{cp} (°C)
PB	121.48	125	19.25	32.7826	7.604	117.60	116
PB2	121.20	126.5	26.07	44.3971	25.16	117.01	115.39
PB215	121.94	128	27.00	45.9809	25.42	117.12	115.47

DOI 10.1002/pc

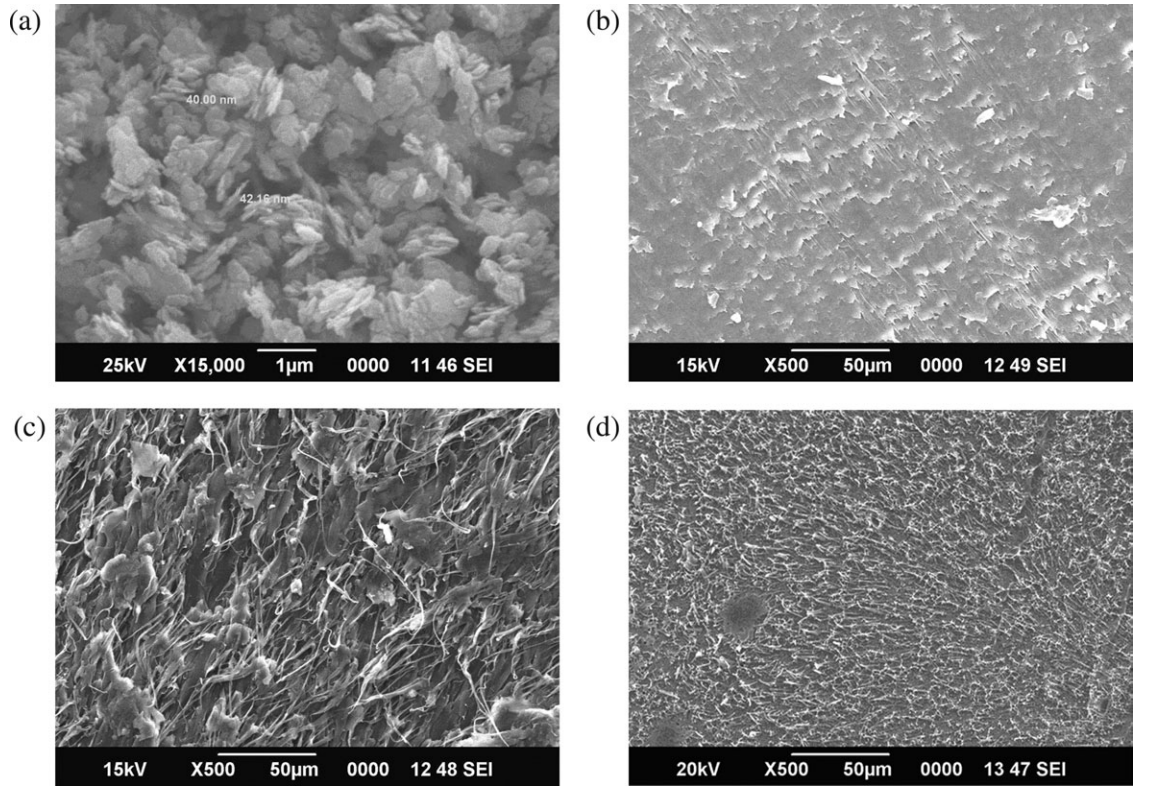

FIG. 12. SEM micrographs (a) kaolin clay, (b) PB, (c) PB2, and (d) PB215.

properties is brought by morphology change, as documented in the Fig. 12 showing SEM micrographs. Figure 12a shows the SEM micrograph of kaolin clay. The fractured surface of the PB, Fig. 12b, is relatively smooth with macro morphology of the propagation crack region marked mainly by the presence of tears, indicating a brittle failure. It exhibits no signs of plastic deformation or drawing. With increasing the magnification, the fracture surface becomes smooth and featureless. In contrast, the nanocomposite with incorporated clay shows a clear evidence of plastic deformation. The fractured surfaces were full of extensive matrix fibrils. The addition of clay drastically changes the fracture mechanism and overall surface morphology. On the fractured surface of PB2, Fig. 12c, it is possible to see fibrils, which seems to connect different domains, indicating that material has been plastically deformed. It is clearly seen that the adhesion between PS and HDPE is improved. Moreover, most of the PS particles were settled or linked by the fiber of the PE matrix, which was due to clay appearing to span the interface between regions of PS/PE blend [47]. The improvement of fineness and uniformity of the compatibilized samples are quite evident on comparing PB2 with PB215. As shown in Fig. 12d, the whole surface of PB215 is covered with fibrils suggesting that the sample undergoes plastic deformation and that a ductile fracture mechanism is active (shear yielding). This may be due to better interfacial interaction and the dissipation of energy through matrix stretching as evidenced by Zhang and coworker. A similar morphological nanocomposite was obtained by them [48]. In the case of compatibilized samples due to the strong interfacial adhesion between dispersed phase and the matrix phase, breakage of PE particles occurred after their yielding followed by plastic deformation. The fibrillar structure of the PE phase generated by loading is obvious. Occurrence of this type of deformation (yielding followed by strain hardening) in compatibilized samples consumes more energy [49].

CONCLUSIONS

Nanokaolin clay can act as an efficient reinforcing agent for the PS/HDPE blends. Mechanical properties improved with an optimum of 2 wt% of clay. The improvement in mechanical properties with kaolin clay is moderate. The improvement becomes significant in the presence of a compatibilizing agent at 10–15 wt%. The tensile strength and tensile modulus of compatibilized blends increase by 18 and 10%, respectively as compared to the neat matrix. XRD results revealed the formation of nanocomposite as the nanoclay was intercalated. The storage modulus of compatibilized blends is much greater than the modulus of neat matrix. DSC data show an increase in melting temperature of the compatibilized nanocomposite. SEM analysis shows the development of fibrillar morphology by the incorporation of clay. The fractured surfaces of the composites show plastic deformation owing to the incorporation of clay. These demon-

strated the sufficient interfacial interaction between the matrix phases.

REFERENCES

1. E.P. Giannelis, *Adv. Mater.*, **8**, 292 (1996).
2. J. Pinnavaia and G.W. Beall, *Polymer Nanocomposites*, Wiley, New York (2000).
3. J. Meng and X. Hu, *Polymer*, **45**, 9011 (2004).
4. L.A. Utracki, *Commercial Polymer Blend*, Chapman and Hall, London (1998).
5. B. Xu, J. Simonsen, and W.E. Rocheford, *J. Appl. Polym. Sci.*, **76**, 1100 (2000).
6. R. Krishnamoorthi and R.A. Vaia, *Polymer Nanocomposites: Synthesis and Characterisation, and Modelling*. ACS Symposium Series, Washington DC, 804 (2001).
7. O. Eriksson, M.C. Reich, B. Frostell, A. Bjorklund, G. Assefa, J.O. Sundqvist, J. Granath, A. Baky, and L. Thyselius, *J. Clea. Product.*, **13**, 241 (2005).
8. S.S. Ray, S. Pouliot, M. Bousmina, and L.A. Uttracki, *Polymer*, **45**, 8403 (2004).
9. Y.S. Lipatov, *Prog. Polym. Sci.*, **27**, 1721 (2002).
10. J.S. Hong, Y.K. Kim, K.H. Ahn, and S.J. Lee, *J. Appl. Polym. Sci.*, **108**, 565 (2008).
11. Y. Wang, Q. Zhang, and Q. Fu, *Macromol. Rapid. Commun.*, **24**, 231 (2003).
12. Y. Li and H. Shimizu, *Polymer.*, **45**, 7381 (2004).
13. B.B. Khatua, D.J. Lee, H.Y. Kim, and J.K. Kim, **37**, 2454 (2004).
14. D. Voulgaris and D. Petridis, *Polymer*, **43**, 2213 (2002).
15. M. Balachandran, L.P. Stanly, R. Muraleekrishnan, and S.S. Bhagawan, *J. Appl. Polym. Sci.*, **118**, 3300 (2010).
16. R. Sukumar and A.R.R. Menon, *J. Appl. Polym. Sci.*, **107**, 3476 (2008).
17. P.G. Rouxhet, N. Samudacheata, H. Jacobs, and O. Anton, *Clay Miner.*, **12**, 171 (1977).
18. J.M. Lagaron, D. Cava, L. Cabedo, R. Gavara, and E. Gimenez, *Food. Addit. Contam.*, **22**, 994, (2005).
19. J.E. Gardolinski, L.P. Ramos, P.G. de Souza, and F. Wypych, *J. Colloid Interface Sci.*, **221**, 284 (2000).
20. T.A. Elbokl and C. Detellier, *J. Colloid Interface Sci.*, **323**, 338 (2008).
21. T.A. Elbokl and C. Detellier, *Can. J. Chem.*, **87**, 272 (2009).
22. B. Chen and J.R.G. Evans, *Carbohydr. Polym.*, **61**, 455 (2005).
23. N.M. Ahmed, D.E. El-Nashar, and S.L. Abd El-Messieh, *Mater. Des.*, **32**, 170 (2011).
24. S. Zhao, S. Qiu, Y. Zheng, L. Cheng, and Y. Guo, *Mater. Des.*, **32**, 957 (2011).
25. C. Sanchez, B. Julian, P. Belleville, and M. Popall, *J. Mater. Chem.*, **15**, 3559 (2005).
26. A. Okada and A. Usuki, *Macromol. Mater. Eng.*, **291**, 1449 (2006).
27. H. Zhao, K. Robert, and Y. Li, *Polymer*, **47**, 3207 (2006).
28. V. Svehlov and E. Polouek, *Angew. Makromol. Chem.*, **214**, 91 (1994).
29. H. Akita and T. Hattori, *J. Polym. Sci. B: Polym. Phys.*, **37**, 189 (1999).
30. H. Akita and H. Kobayashi, *J. Polym. Sci. B: Polym. Phys.*, **37**, 209 (1999).
31. J.H. Chang and Y.U. An, *J. Polym. Sci. B: Polym. Phys.*, **40**, 670 (2002).
32. J. Wang, S.J. Severts, and H.P. Geil, *Mater. Sci. Eng. A.*, **467**, 172 (2007).
33. X. Zhang and L.S. Loo, *J. Polym. Sci. B: Polym. Phys.*, **46**, 2605 (2008).
34. C.J. Hung, H.Y. Chuang, and F.C. Chang, *J. Appl. Polym. Sci.*, **107**, 831 (2008).
35. E.P. Ayswarya, B.T. Abraham, and E.T. Thachil, *J. Appl. Polym. Sci.*, **124**, 1659 (2012).
36. M.Z. Rong, M.Q. Zhang, Y.X. Zheng, H.M. Zheng, R. Walter, and K.P. Friedrich, *Polymer*, **42**, 167 (2001).
37. J. Johns and V. Rao, *Fibers Polym.*, **10**, 761 (2009).
38. T. Yong and H. Yuan, *Polym. Adv. Technol.*, **14**, 733 (2003).
39. P.H. Nam, P. Maiti, M. Okamato, T. Kotaka, N. Hasegawa, and A. Usuki, *Polymer.*, **42**, 9633 (2001).
40. J.W. Gilman, C.L. Jackson, A.B. Morgan, and R. Harris, *Chem. Mater.*, **12**, 1866 (2000).
41. V. Krikorian and D.J. Pochan, *Macromolecules.*, **37**, 6480 (2004).
42. P. Svoboda, Z. Ch, H. Wang, L.J. Lee, and D.L. Tomasko, *J. Appl. Polym. Sci.*, **85**, 1562 (2002).
43. S.M. Ali Dadfar, I. Alemzadeh, S.M. Reza Dadfar, and M. Vosoughi, *Mater. Des.*, **32**, 1806 (2011).
44. N. Ning, F. Luo, K. Wang, Q. Zhang, F. Chen, R. Du, C.Y. An, *J. Phys. Chem. B.*, **112**, 14140 (2008).
45. S. Akhlaghi, A. Ali, M. Sharif, A. Kalaee, A. Elahi, and M.P.S. Afshari, *Mater. Des.*, **33**, 273 (2012).
46. F. Perin-Sarazin, M.T. Ton-That, M.N. Bureau, and J. Denault, *Polymer*, **46**, 11624 (2005).
47. N. Wanga, N. Gaol, Q. Fang, and E. Chen, *Mater. Des.*, **32**, 1222 (2011).
48. N. Wang, M. Li, and J. Zhang, *Mater. Lett.*, **59**, 2685 (2005).
49. M. Khodabandelou, M.K.R. Aghjeh, and M. Rezaei, *Eng. Fract. Mech.*, **76**, 2856 (2004).

 DOI 10.1002/pc